Time-resolved diagnostics of a pin-to-pin pulsed discharge in water: pre-breakdown and breakdown analysis

C. Rond, J.M. Desse, N. Fagnon, X. Aubert, M. Er, A. Vega, X. Duten

Time-resolved diagnostics of a pin-to-pin pulsed discharge in water: pre-breakdown and breakdown analysis

C. Rond [1,a], J.M. Desse[2] , N. Fagnon[1], X. Aubert[1], M. Er[1], A. Vega[1] and X. Duten[1]

[1]*LSPM - CNRS UPR3407, Université Paris 13,Villetaneuse, 93430, France*

[2]*ONERA - Department of Applied Aerodynamics, 5 Boulevard Paul Painlevé, BP 21261, 59014 LILLE Cedex, France*

Abstract. This paper presents an experimental study of an underwater pulsed plasma discharge in pin-to-pin electrode configuration. Time resolved refractive index-based techniques and electrical measurements have been performed in order to study the pre-breakdown and breakdown phenomena in water. A single high voltage pulse with amplitude of a dozen of kV and duration of [0.1-1] ms is applied between two 100 µm diameter platinum tips separated by 2 mm. This novel experimental work reports that different cases of electrical discharge in water occurs for a unique set of experimental conditions such as (i) bush-like channels from the cathode that do not span the electrode gap, (ii) bush-like channels from the cathode leading to breakdown and (iii) filamentary structures from the anode leading to a stronger breakdown. Two breakdown mechanisms, anode and cathode regimes, have been clearly identified and related to the two principal schools of thoughts to explain discharge propagation in liquid.

1. Introduction

Attention in the electrical breakdown in liquids starts from dielectric liquid applications such as high-voltage transformers or switches (1-3). The study of electric discharges in water, which has higher permittivity and conductivity than dielectric liquids, is more recent and arises in the frame of applications such as nanomaterial synthesis (4-7) and environmental applications (8-12) owing to high generation of active species. Despite the increasing interest in the last years, the physical and chemical mechanisms involved in the initiation and the propagation of the discharge in water remain not well understood (13-15). The main difficulties for the comprehension of plasma-liquid processes are the nanosecond timescale and the multiphase type of the involved phenomena, which allows only a few numbers of appropriate diagnostics. Whereas the interpretation of optical emission spectroscopy results remains sensitive (16-18), time resolved refractive index-based techniques and electrical measurements are known to be reliable and complementary diagnostics in the field of plasma-liquid (1, 15, 19).

The literature highlights two theories to explain breakdown in liquid: the low density region theory where a gas phase is precursor to the avalanche process and the direct impact ionization model in the liquid state itself which results in a charge

[a] Author to whom correspondence should be addressed. Electronic mail: rond@lspm.cnrs.fr

carrier multiplication (20-23). Although recent studies have demonstrated the possibility of direct electron impact ionization of water using very short voltage pulses (24, 25), most experimental results have evidenced that low density regions are necessary to make the electron multiplication possible (15, 23, 26, 27).

Pulsed electrical discharge using mainly pin-to-plane electrodes configuration has been widely studied in mineral oil first (28-32). These reference works provide first features of pre-breakdown and breakdown in liquids. Gaseous channels (also called streamers by analogy with gas discharge) develop continuously and discharges occur within the gas phase. The streamers are characterized by different structures according to the polarity: negative streamers which are slow and bushy emanate from the point cathode and positive streamers which are filamentary and fast develop from the point anode. Different modes (4 cathode modes and 3 anode modes) have been identified regarding the velocity and the shape of the streamers (28). The shape of the streamers informs about the degree of non-equilibrium between the streamer and the surrounding liquid . The spherical shape of positive streamer corresponds to a quasi-equilibrium unlike the bush-like negative streamers (15). The transition between modes was mainly observed by changing the experimental conditions, *e.g*. the applied voltage, but two modes can also appear randomly for a given voltage (15, 33).

In the same way, first investigations of underwater pulsed discharge have been widely performed using the pin-to-plane electrode configuration (15, 21, 23, 24, 34-41). As observed for dielectric liquid, the applied voltage polarity leads to very different discharges. Positive streamers have been more studied than negative ones because of their lower breakdown voltage (42). These investigations do not converge on a unique description of the discharge propagation in water because of the influence of numerous parameters (23). For example at low conductivity (0.05 µS/cm), two types of positive streamers in water have been observed by varying the applied voltage (36, 43) whereas at higher conductivity (5 µS/cm), three distinct forms of discharge development have been monitored for various voltages. Without claiming to be exhaustive, other electrodes configuration have been more rarely reported. Electrical discharge in water between plate-to-plate electrodes has been studied but this configuration, involving a low electric field, requires assistance such as shock wave or nitrogen bubble injection (44, 45). Study of pin-to-wire configuration has reported three modes (bubble, bush-like and tree-like) with different sizes and dynamic behaviors according to the deposited energy (25, 33). Two types of pulsed corona discharge have been investigated using pin-to-plate and coaxial electrodes (11, 46). Lastly, pin-to-pin discharge in liquid has been used to synthesize nanoparticles involving two different operation regimes, a glow discharge and an arc discharge, by changing the applied voltage (47, 48). Recently, several experiments of pin-to-pin discharges using bubbles in water have been reported (49-51). These systems present some interesting advantages as a reduction of the energy consumption and a larger contact

area but they involve more complex set-ups to control gas circulation and bubble sizing. It is worth noting that the addition of gaseous bubbles to pin-to-pin discharges involve strong modifications of the system since the electric field intensity required to initiate the breakdown is much lower in gas than in liquid. In these conditions, the ignition of the discharge is controlled by the gas phase.

Possible physical mechanisms involved in streamer initiation and propagation in water have been deeply discussed in (23, 26, 27) concluding that discharges in liquid require low density localized regions. The creation of these regions, *i.e.* the streamer initiation, comes from vaporization, molecular dissociation or mechanical movements. Furthermore general discussion looks after the polarity effect observed on asymmetric geometries such as pin-to-plane electrode configuration. Experimentally the comparison between positive and negative streamers shows that positive streamers are created earlier, are faster and show a filamentary structure whereas the negative streamers appear later, are slower and present a bushy structure. These studies have mostly focused on the pre-breakdown phenomena showing that the propagation modes of the discharge strongly depend on experimental conditions, especially the electrode configuration, the liquid composition and the applied voltage.

The complete understanding of discharge mechanisms in liquids requires more experimental observations, in particular involving new experimental conditions such as the electrode geometry, the electric field or the liquid conductivity. It is worth noting that the literature does not report a detailed experimental study of pin-to-pin discharges in water. Furthermore previous studies used to work with repeated pulse regime of the discharge which involves strong modifications in the liquid such as bubbles formation, liquid composition, hydrodynamic effects and shock wave. As a consequence, the study of repeated pulses regime, even at low frequency, implies that the initial conditions of the system are different for each pulse. Lastly most works have carried out measurements on successive streamers using variable delay to reconstruct the time evolution of the discharge (24, 39, 40). This approach gives a good time resolution (ns) but involves experimental uncertainties because the electrical discharge structure is not perfectly reproducible from one discharge to another. As a consequence, it is necessary to perform time-resolved measurements on a single pulse discharge in order to maintain constant the initial conditions of the experiments, ensuring a higher reproducibility, and to correlate the different parameters measured on a discharge.

This work presents the study of single pulse electrical discharges in water with pin-to-pin electrodes configuration. New experimental results aims at describing different discharge regimes in order to describe, understand and then master the process. In this paper, we report synchronized measurements on a single discharge using both time-resolved optical techniques (schlieren imaging and shadowgraphy) and electrical measurements which are useful complementary diagnostics allowing valuable investigation of both the pre-breakdown and the breakdown stages. The experimental set-up is presented; then the results obtained by time-resolved optical techniques are described. The following section proposes a quantitative

time analysis of the electrical signal. The last section presents a discussion based on comparison between the results of both diagnostics and helped with works on point-to-plane geometry.

2. Experimental set-up

The test cell consists of a 100-mm-long, 45-mm-wide and 50-mm-high polymethyl methacrylate block containing two fused silica windows (Fig.1). Both electrodes are 100 µm-diameter platinum wires encapsulated in a dielectric capillary tube, except for the 0.5 mm-long tip. They are placed in a horizontal pin-to-pin configuration with a gap distance of 2 mm. The pulse generator consists of a 1 nF capacitor charged by a 30 kV high voltage power supply (Ultravolt 30A24-P30) through a ballast resistor of 30 kΩ and discharged by a fast high voltage solid-state switch (Behlke HTS 301-03-GSM). Positive high voltages mono-pulses with rise time of about 30 ns, adjustable duration from 100 µs to 1 ms and amplitude from 6 to 14 kV are produced. The electrical measurements are achieved using a Tektronix high voltage probe connected to the high voltage electrode and a coaxial current shunt (R = 10 Ω) connected to the low potential electrode. Both signals are recorded simultaneously with a 1 GHz Oscilloscope (Lecroy HDO9104). The electrical connections as well as the probes are armored by flexible tubes and shielding boxes in order to minimize the parasitic noise (2). Regarding the optical diagnostics, a 300 W Xenon light source is focused by a condensing 7-lenses system on to a slit and then brought to a parallel beam by a 100 mm focal lens to pass through the test cell. The light is then refocused by a 250 mm lens, in the plane of a knife edge for schlieren measurements, while the region of interest of the test cell (interelectrode gap) is focused by a 200 mm lens on the sensor of a high speed camera (Phantom V1210). Videos have been recorded using two different parameter sets: an exposure time of 0.91 µs and a widescreen resolution of 128x32 pixels which allows 571 500 frames per second; an exposure time of 0.56 µs with a widescreen resolution of 128x128 pixels which allows 240 600 frames per second. It is worth noting that the camera allows monitoring both variation of the refractive index and strong light emissions. The experiments were performed in a mixture of de-ionized water and sodium chloride in order to keep the conductivity constant at σ=100 µS/cm.

Special attention was paid to maintain constant the initial conditions of the discharge, in particular the time between two measurements was high enough to avoid residual bubbles. Moreover hundreds of measurements have been carried out for each experimental condition in order to ensure the reproducibility of the observed phenomena and to provide reliable analysis of the results. Furthermore we specify that the monitoring of the results do not present any time evolution which could be due to experimental set-up modifications such as strong modifications of the electrodes.

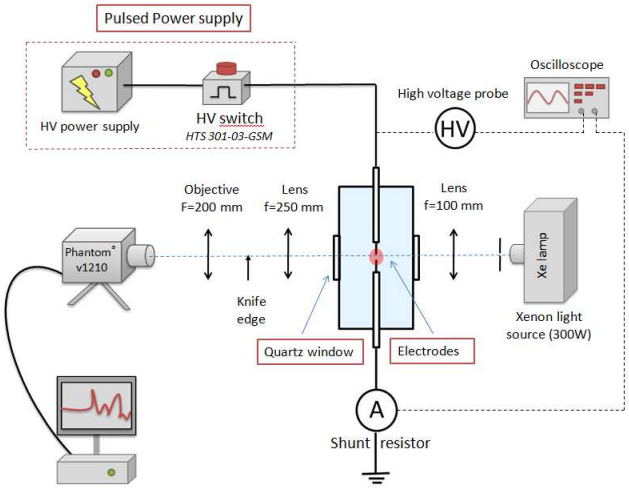

FIG. 1. Schematic diagram (top view) of experimental apparatus showing pulsed power supply, test cell, electrical probes and schlieren setup (same set up for shadowgraphy except the knife edge)

3. Discharge description

Density gradients of a transparent medium are made visible by optical techniques as schlieren and shadowgraphy thanks to small changes in the index of refraction of the fluid (52). Refraction effects initiated by pulsed discharge in liquid can be due to region of low density or channels filled with gas (23, 53). Refractive index techniques mainly involve qualitative analysis of the phenomena. In this study the use of both shadowgraphy and schlieren provides complementary results which constitute a reliable indicator of phase change. Moreover in order to improve the sensitivity of the techniques, a very intense light source is used which makes it impossible to detect possible low emission, only very strong emissions can be observed.

Considering all experimental results of this work, three different cases of discharge have been identified and described by time-resolved refractive index-based techniques. The interesting features of each case are shown on Fig. 2. It is worth noting that different cases can be observed for a unique set of experimental conditions. A statistical analysis shows that for 9 kV 5% of case 1 and 95% of case 2 have been monitored and for 12 kV 90% of case 2 and 10% of case 3 have been observed.

Cases 1 and 2 show bush-like structures that propagate from the cathode to the anode whereas case 3 depicts a filamentary structure that emerges from the anode. In case 1 (Fig. 2a), few microseconds after the voltage pulse, low variations of the refractive index are observed at both electrode tips (from 3.5 to 43.75µs). These regions, cone-shaped at the cathode and spherical at the anode, highlight low variations of the fluid density. Then after a time of about a hundred of microseconds, bush-like dark channels are forming principally at the cathode (starting @ 96.25µs). These channels, most probably filled

with gas resulting from the vaporization of the water propagate slowly towards the anode but do not span the interelectrode gap (@ 126µs). This case is called partial electrical discharge (22). The propagation of the channels from the cathode is slow ($v_{1,c}$ ≈5 m/s), lasts during less than 100 µs and then results mainly in bubbles and convective motion of the fluid (not shown in Fig.2).

In case 2 (Fig. 2b for 9kV and Fig.2c for 12kV), initial variations of the fluid density can also be observed at each electrode tip but the dark channels appear more rapidly at the cathode (@ 14µs on Fig 2b and @ 7µs on Fig 2c) and a dark phase is also present at the anode. Whereas the dark phase at the anode expands more spherically and slowly ($v_{2,a}$ ≈15 m/s), channels propagate from the cathode (to the anode) with a bushy structure and a higher velocity than in case 1 (v_2≈50 m/s). Channels cross the interelectrode gap being either not luminescent (@ 42 µs on Fig 2b) or luminescent (@ 19.25 µs on Fig 2c) which leads to the breakdown phenomena. As a consequence an intense light is emitted from the dark region (@ 21 µs on Fig 2c) which suggests that a strong excitation occurs. Next the dark region expands in a spherical shape (v ≈10m/s) and contracts several times (oscillations, not shown on Fig 2). Following the breakdown phenomena, one, two or three secondary emissions can be observed in the dark phase (@ 126 µs on Fig.2c). As a consequence we define for each experiment the number of breakdowns generated by a single discharge (from 1 to 4) and the time position (rank) of the breakdown (1^{st}, 2^{nd}, 3^{rd} or 4^{th}). A statistical analysis shows that for 9 kV 70% of discharges involve 1 breakdown and 30% of discharges involve 2 breakdowns; for 12 kV discharges corresponding to case 2 are shared between 2, 3 and 4 breakdowns at 33%, 50% and 17% respectively.

Regarding case 3 (Fig.2d), a filamentary structure initiates and propagates from the anode toward the cathode at a higher velocity (v_3>400 m/s, only a low threshold can be measured because of the camera properties) (@ 3.5µs). Contrary to case 1 and case 2, no dark region has been observed at the cathode before the channel spans the gap. This analysis remains sensitive since the characteristic time of the phenomena is close to the time resolution of the camera (1.75 µs). Light emission can be observed during the propagation of the channels and a very intense emission is produced when the filament spans the interelectrode gap (@5.25µs). Upon the breakdown phenomena, a circular shock wave is produced propagating away the gap (not shown in Fig.2d). Several secondary emissions systematically occur (*e.g.* @ 22.75µs) and the dark phase expands spherically (v ≈10m/s). A region of low refractive index appears in the center of the dark phase which indicates local low pressure due to the expansion (from 42 to 126 µs). As discussed previously, these low refractive index regions cannot be mistaken with low emission, this result has been confirmed by time-resolved optical emission measurements (to be

published). Then the dark volume decreases and implodes which results in a new shock wave formation (not shown in Fig.2d).

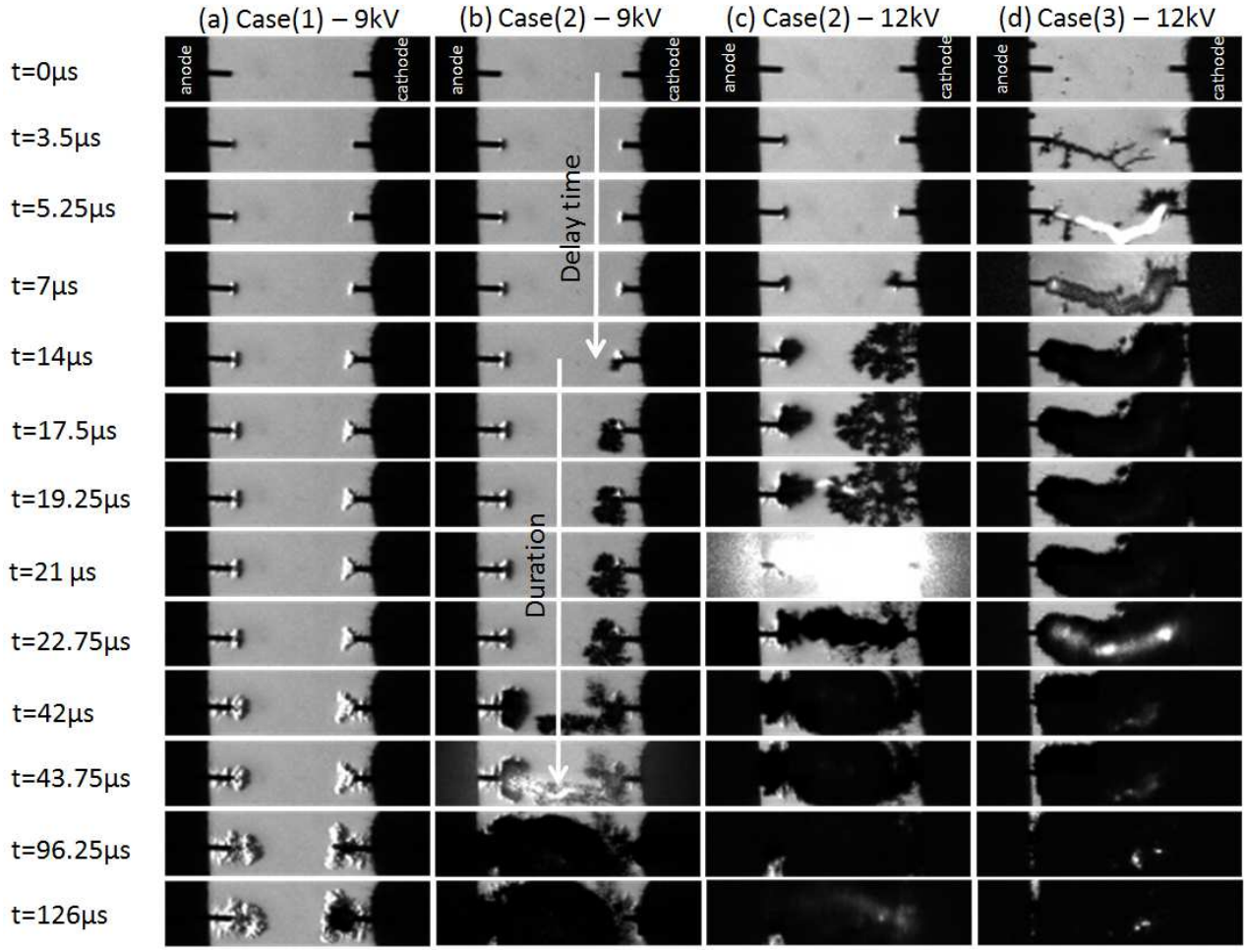

FIG. 2. Time resolved schlieren measurements of a pin-to-pin discharge obtained in water (σ=100µS/cm) for 9kV and 12 kV - the voltage pulse duration equals 1 ms and the camera resolutions are 128x32 pixels and Δt=1.75 µs.

4. Electrical signals

In Fig. 3 typical traces of the time evolution of the voltage and the current monitored for the three cases are shown for a pulse duration of 500 µs. Following the pulse (rise time of about 30 ns), the voltage decreases slowly when the current increases up to 100 mA during first microseconds. The very beginning of the discharge (<15 µs) is similar for all cases.

Then for case 1 the signals show three consecutive sequences (Fig.3a): (1) low variations of the electrical signals, the voltage continues decreasing close to an exponential and the current is about one hundred of milliamps before decreasing slowly; (2) after about 100 µs, voltage signal shows a slope change and a transient current showing rapid alternative positive and

negative values overlaps the slowly varying current; (3) finally both the voltage and the current signals decrease slowly. The global shape of the electrical signals is very similar to the characteristic voltage and current traces of RLC circuit with an overdamped response. As a consequence we defined the slowly varying current as *RLC current* and the alternative current as a *transient current.*

Regarding case 2, from about 15 µs the voltage signal decays faster (than case 1) and the current waveform shows a high transient current (Fig.3). Then the capacitor bank is discharged suddenly by the breakdown phenomena characterized by a voltage drop of few kV and simultaneously a peak current of more than 20 amps. Next, large pulse duration allows the capacitor to charge again and the voltage increases slowly with a RC time constant equal to τ=30µs. Afterwards either (i) the voltage signal decays with the current close to zero (Fig. 3a) or (ii) one or more additional breakdown phenomena occur (2 additional breakdowns are shown on Fig. 3b). It is to notice that no transient current has been recorded before secondary peak currents. Fig.4 presents a magnification of the current trace of CASE 2 from Fig.3b where RLC current, transient current and breakdown current peaks are clearly identified.

For case 3 the breakdown phenomena happens faster than for case 2 and no transient current but only the RLC current appears during the pre-breakdown (see insert in Fig. 3b). After the first capacitor discharge, several successive breakdown phenomena occur (5 additional breakdowns are shown on Fig. 3b) in a similar way of case 2.

It is noted that, for cases 2 and 3, the breakdown voltage drops to a value around 1 kV for the first breakdown and 100 V for secondary breakdowns because of the resistance of the channels that is estimated at about 100 ±50 Ω from the electrical traces for every breakdown.

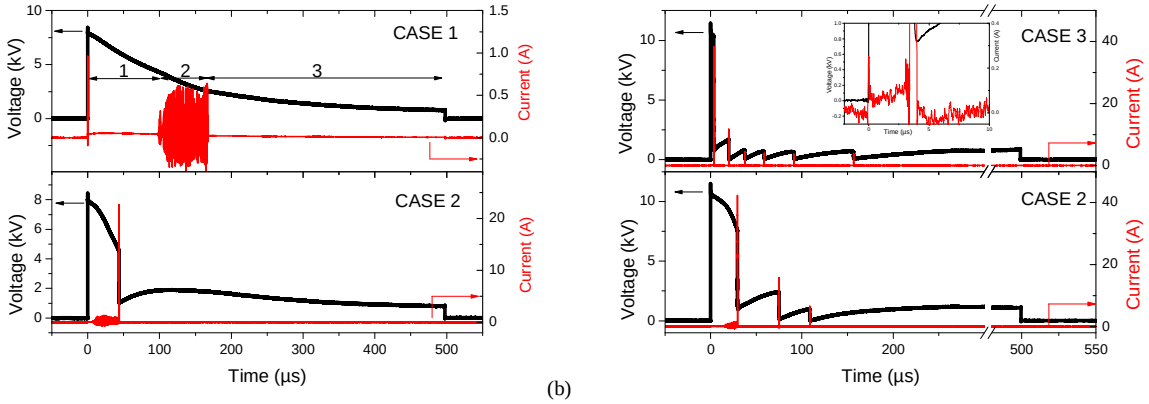

FIG. 3. Voltage and current signals of a pin-to-pin discharge in water (σ=100µS/cm) monitored for applied voltages of (a) 9kV and (b) 12kV. The inserts corresponds to zoom of the signals.

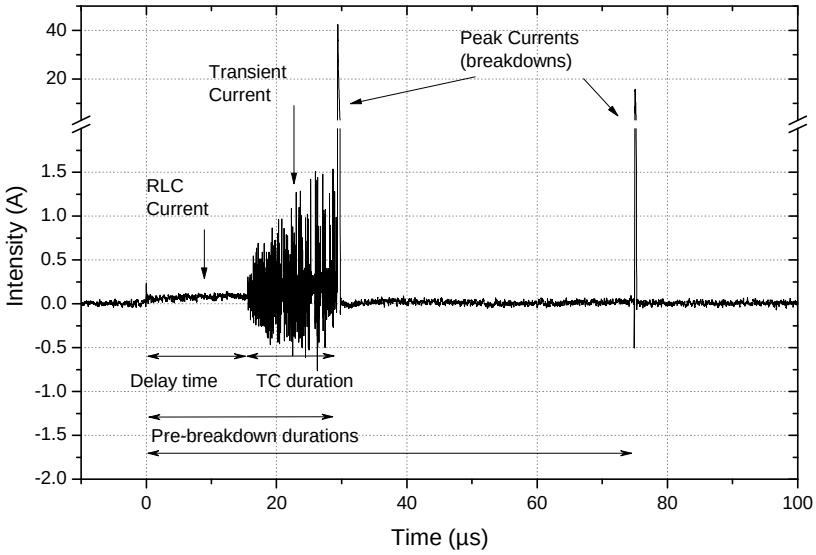

FIG. 4. Magnification of the current signal of the CASE 2 typical trace presented on Fig.3(b)

From these first analyses, two particular regions of interest have been identified as the pre-breakdown and the breakdown. The charge transferred to the liquid can be estimated by either the voltage drop at the measurement capacitor C=10 nF ($Q = C.\,\Delta U$) or by the integration of the current peak on the region of interest ($Q = \int I.dt$). We have estimated the charges involved during the pre-breakdown and the breakdown using these two definitions and the results show very good agreement within 10% of discrepancy between the two methods. The average values of charges are summarized in Tab.1. We have noticed that the charge transferred during the pre-breakdown is mainly due to the RLC current, the contribution of the transient current is negligible. Tab.1 shows that the distribution of the initial amount of the charge into pre-breakdown and breakdown depends on the case. For case 3 5% of the initial charge is transferred during the pre-breakdown whereas pre-breakdown of case 2 involves at least 30%. Furthermore for case 2 we observe a correlation between the number of breakdowns and the charge distribution. When less charge is transferred during the pre-breakdown, a higher amount of charge is involved in the breakdown which induces a higher excitation/ionization of the species and then favors more additional breakdowns. The total charge transferred to the liquid during the first breakdown is equal to the addition of the pre-breakdown and breakdown charges (values in bold in Tab.1). We observed that, whatever the experiment, the total charge does not equal the initial charge, the difference being about 1 µC. This result is in agreement with the observations on voltage traces regarding the minimum value of about 1kV reached following the first breakdown.

The charges transferred during secondary breakdowns are also reported in Tab.1. We note that neither the case nor the number of breakdowns have an influence on the charge since second breakdowns involve about 2 µC and the other ones about 1µC.

Initial Charge (Applied Voltage)		Case 2										Case 3			
		1 Bk	2 Bk		3 Bk			4 Bk							
8 µC (9kV)	Pre-Bk	**4**	**3.2**												
	Bk	**3.4**	**3.8**	1.6											
	Total	**7.4**	**7**												
10.8 µC (12kV)	Pre-Bk		**3.9**		**3.4**			**2.9**				**0.5**			
	Bk		**6.2**	2.1	**6.6**	2.2	1.1	**7**	2	1	1	**9.3**	1.7	0.8	0.7
	Total		**10.1**		**10**			**9.9**				**9.8**			

Tab.1 Mean values of charge (in µC) transferred during the pre-breakdown (Pre-Bk) and the breakdown (Bk) according to the applied voltage (9 & 12 kV), the case and the number of breakdowns. First breakdown charges are written in bold

5. Comments of the results

The comparison of time resolved optical imaging and electric measurements allows a detailed description of the initiation and the propagation of the discharge in water. Both diagnostics have identified three cases for pin-to-pin electrical discharge in water. Among them, we can highlight 2 different regimes which are very similar to results observed for discharges in dielectric liquids using a point-to-plane geometry (54). But these two regimes have been distinguished despite the fact that all the parameters are kept constant whereas previous studies have shown that the breakdown scenario in liquid is driven by the experimental conditions as the applied voltage, the polarity or the pulse duration. In particular for pin-to-plane geometry, the polarity has a strong influence on initiation mechanisms and propagation of streamers (23, 26, 27, 55). The present case 1 and case 2 show common features with the point-to-plane cathode regime in which the heating by Joule effect leads to the liquid vaporization forming bush-like channels at the cathode and to the apparition of a transient current. Case 3 of this work shares peculiarities with the point-to-plane anode regime in which the channels propagate faster and from the anode, neither vaporization nor transient current has been observed during the pre-breakdown but a continuous current. The effect of the polarity is explained because of the difference in mobilities between electrons and ions (23, 26, 27). The initiation mechanisms at the electrodes tip involve different charge transport: the initiation of positive streamers is related to field assisted ionic dissociation and involves ionic transport whereas the initiation of negative streamers by Fowler-Nordheim electron emission involves electron transport. It has been pointed out that positive streamers are thin because of low mobility of ions whereas negative streamers are bushier because of the higher diffusion and mobility of the electrons. This charge

dilution effect has also a consequence on the delay time of streamers since more time is necessary for negative streamer to appear. Furthermore the negative streamer propagation which depends on electrons drift is slower than the positive streamers propagation since in the latter case the low ion mobility involves a local field enhancement at the streamer head which exponentially enhances the rate of field ionization. Finally, the luminosity of positive streamers is higher because the probability of radiative recombination is higher for mechanisms involving electrons flowing back in the filament where ions density is important than for electrons produced by negative streamers and recombining with ions in the bulk.

By analogy the two regimes described in this work are called *cathode regime*, including case 1 and case 2, and *anode regime* for case 3, even if the polarity has not been changed.

Pre-breakdown phase

Regarding the cathode regime, two characteristic times of the pre-breakdown have been defined. On the one hand the delay time is defined as the time needed for the appearance of the dark phase on the refractive index imaging (illustrated in Fig.2b) as well as the time corresponding to the beginning of the transient current on the electrical signal (sequence 1 in Fig.3). On the other hand the duration corresponds to the duration of the transient current (TC duration) measured on the electrical trace (sequence 2 in Fig.3) and the duration of the dark phase expansion estimated from imaging (illustrated in Fig. 2b). Average values have been estimated from dozen of experiments carried out in same experimental conditions. The mean delay time and the mean duration are reported on Fig. 5. The error bars are used to represent the dispersion of the results obtained in same conditions since the uncertainties defined by the sensitivity of the detectors are lower.

The agreement between the measurements obtained with both diagnostics is very good. We observe that the transient current appears with the dark phase and exists as long as this phase is produced at the cathode. This correlation suggests that, as in pin-to-point configuration, the RLC current involves the formation of a gas phase (dark phase) where charged species are produced. The delay time of vaporization depends on the case since the time needed for the gas phase to appear in case 1 is about 100 µs whereas it is close to 10 µs in case 2. Then for case 1 the mean delay time is about ten times higher than in case 2. In term of energy, defined as the current-voltage product integrated over the time, we also obtain this factor of ten, with an energy deposited over the delay time equal to about 30 mJ in case 1 and 3 mJ in case 2, since measurements of the RLC current show same results for both cases. Thus, although the initiation and the propagation mechanisms observed by imaging look similar, we report a high variation of the deposited energy measured at the very beginning of the vaporization. As a consequence the formation of the gas phase cannot be explained by the only Joule effect if we consider that initial conditions are identical between case 1 and case 2. Either other additional processes are involved in the initiation of the

vaporization (as Fowler-Nordheim electron emission) or the initial micro-properties of the fluid are more different than expected (as micro-bubbles presence) (26).

Moreover we report on Fig. 5 that for case 1 the transient current duration is about 65 µs whereas it ranges between 10 and 35 µs for case 2. It means that the channels propagation is faster for case 2 than for case 1.

The comparison between case 1 (no breakdown) and case 2 (breakdown) aims to identify the conditions allowing the breakdown. For case 1 when the vaporization occurs, the voltage has significantly decreased and the electric field is not high enough to sustain the discharge, the channel propagation is slow and no breakdown occurs. The initiation of the gas phase plays an important role on the time evolution of the discharge. For the cathode regime the voltage required to initiate the streamer is lower than the voltage required for its propagation to breakdown: the propagation mechanisms control the breakdown. On the contrary, for the anode regime every streamer leads to breakdown so the initiation mechanisms control the first breakdown (15, 29).

"Moreover, the anode regime (case 3) does not show any transient current or dark phase at the cathode during the pre-breakdown. This concordance demonstrates that no gaseous phase has been formed at the cathode during the pre-breakdown of case(3). Furthermore it is to notice that no transient current has been monitored before secondary breakdowns of case 2 and case 3. These breakdowns occur in a gas phase that already exists which suggests that the transient current is not characteristic of the gas ionization but of the liquid vaporization process at the cathode.

The RLC current of case 3 is very similar to the measurements of the cathode regime but on a shorter period which leads to a lower pre-breakdown charge (Tab.1). Following the first breakdown, up to 3 additional breakdowns could occur for cathode regime whereas several additional breakdowns systematically occur for anode regime. The anode regime is more efficient to transfer charges during the breakdown process which results in higher gas excitation and then easier gas re-excitation.

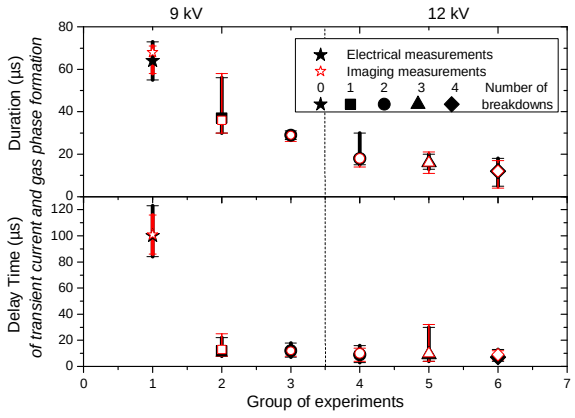

(a)

Fig 5 Delay time and duration of transient current and gas phase formation measured using the current traces (filled symbols) and time-resolved refractive index-based techniques (open symbols) - the symbols represent the mean value recorded for same experimental conditions and the bars indicates the dispersion of the measurements. The symbol shape informs about the total number of breakdowns occurring during the discharge.

Breakdown process

As explained previously, only experiments of case 2 (cathode regime) and case 3 (anode regime) are involved in this section. When the gas channels span the interelectrode gap, a high current peak is recorded. The current corresponds to high electron flux in the gas channel that causes the high excitation of the molecules which results in a strong emission. The pre-breakdown duration is defined as the time for the channels to span the gap. On imaging measurements, this time corresponds to the connection of the gas phases arisen from the electrodes and/or the emission of visible light. On electrical measurements this time corresponds to the voltage drop (or current peak). We point out that the pre-breakdown duration of case 2 corresponds to the sum of the delay time and the duration of the transient current (shown in Fig. 4).

After the first breakdown, the gas phase between the electrodes expands due to pressure effect and the capacitor loads again because of the large pulse duration. Then both the decrease of the pressure of the gas phase and the increase of the voltage can lead to secondary breakdowns (as predicted by the Paschen curve approach for homogeneous electric field). These phenomena result in new current peaks and light emissions. Therefore by extension, pre-breakdown duration can also be estimated for these secondary breakdowns considering the time of each secondary emissions to occur (when observed) and the corresponding time of voltage drop (or current peak). Measurements of pre-breakdown duration have been performed for case 2 and case 3 using the two methods and the results are shown in Fig 6a. The agreement is very good between electrical and imaging measurements confirming that the light emission, the voltage breakdown and the current peak occur simultaneously. For case 2 the experiments have been distinguished according to the number of breakdowns during the discharge (from 1 to 4) whereas results of case 3 do not present such a degree of details.

The results of case 2 show that the number of breakdowns increases when the pre-breakdown duration of the first breakdown decreases. That is consistent with the discussion about the effect of the transferred charge (Tab.1). It is interesting to notice that the pre-breakdown duration of secondary breakdowns also decreases when the number of breakdowns increases. Moreover first pre-breakdown duration of case 3 ($\approx 5\,\mu s$) is lower than those of case 2 ($>10\mu s$) which means that the initiation and/or propagation mechanisms involved in anode regime are faster than in cathode regime. As a consequence, high propagation velocity of the channels involves a shorter total duration of the RLC current, so a lower pre-breakdown charge.

Therefore as already mentioned, higher charge is transferred during the breakdown which leads to a higher excitation of the medium and then more and faster secondary breakdowns.

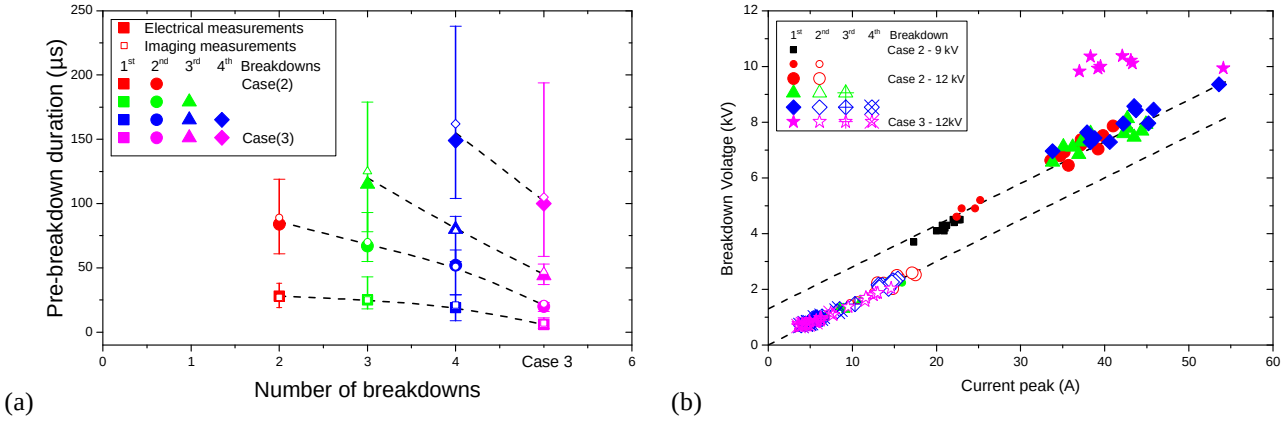

Fig 6 (a) Pre-breakdown duration according to number of breakdowns and case, measured at U=12kV using the electrical traces (filled symbols) and time-resolved refractive index-based techniques (open symbols) - the symbols represent the mean value recorded for same experimental conditions and the bars indicates the dispersion of the measurements (b) Breakdown voltage according to current peak measured at U=9kV (small symbols) and U=12kV (large symbols).

The equivalent electrical circuit of a liquid used to be defined as a resistance in parallel with a capacitor, the inductance is not considered. The Maxwell relaxation time ($\tau=\varepsilon/\sigma$) allows to identify the resistive or capacitive behavior of the liquid. The water conductivity (100 µS/cm) involves a relaxation time of 70 ns that is less than the propagation time (several µs) which indicates a resistive behavior of the liquid during the discharge (15, 38). As a consequence the breakdown current-voltage (I-V) characteristic represents an interesting tool to highlight the discharge regimes. Fig 6(b) shows the breakdown voltage in relation with the peak current for two applied voltages (9 and 12 kV). The measurements can be divided into three groups:

(a) First breakdowns of case 3 are lined up along a horizontal line satisfying the equation $U=E_a$, where E_a equals about 10 kV. In this configuration, the voltage remains constant (≈10kV) and the current values are high, ranging in [35-55] A.

(b) First breakdowns of case 2 show high voltage (4-9 kV) and high current (20-45 A). These measurements are lined up along a straight line not passing through the origin. The experiments satisfy the equation $U=R_b.i + E_b$ with $R_b \approx 150\ \Omega$ and E_b a threshold voltage equals to 1.3 kV. The number of breakdowns seems to have an influence for 9 kV but not for 12 kV.

(c) Secondary breakdowns of cases 2 and 3 (unfilled symbols) are defined by lower values of voltage (<3kV) and current (<20A). The electric signal measurements corresponding to the 2nd, 3rd and 4th breakdowns are lined up along a straight line parallel to the previous one but passing through the origin. The experiments satisfy the equation $U=R_c.i$ with $R_c \approx 150\ \Omega$. The number of breakdowns does not have a significant influence on the current-voltage function. However the rank of the

breakdown has an influence since the couple current-voltage decreases when the rank increases. These results are consistent with the value of the charge presented in Tab.1.

On the one hand, these results suggest that mechanisms responsible for secondary breakdowns are similar whatever the regime. The secondary breakdowns result from electrons flow in the gas phase that has been previously formed by the 1st breakdown. The resistance R_c (150 Ω) is then a characteristic of the electrical properties of the gas phase. It means that the 1st breakdown of the two regimes leads to the creation of a gas phase with comparable properties (composition, pressure, temperature). The charge of the capacitor is also similar so the mechanisms associated to secondary streamers propagation are the same.

On the other hand, the breakdown current-voltage (I/V) characteristic suggests different mechanisms responsible for the first breakdown according to the regime. The slope of the (I/V) characteristic for first breakdowns of case 2 is the same that those of secondary breakdowns (R_b=R_c≈150Ω). We can conclude that the current peak of case 2 is due to charges transfer in a gas phase. This result confirms the formation of a gas phase prior to the first breakdown in the frame of cathode regime. However, the intercept of the line is different. Contrary to secondary breakdowns, the (I/V) characteristic of first breakdowns shows a threshold voltage (1.3 kV). This value can be related to the vaporization necessary for the first breakdown, and so it is characteristic to the liquid properties.

The slope of the (I/V) characteristic for first breakdowns of case 3 is different to the previous one. Then we cannot conclude about any vaporization process related to the anode regime. The results show that a threshold voltage of about 10 kV is required to initiate the first breakdown. It confirms that for the anode regime every streamer leads to breakdown so the initiation controls the first breakdown. Whereas we observed a variation in the current peak value (from 35 to 55 A), the charge is constant (≈9µF). It involves variations in current propagation that can be due to inhomogeneity in the liquid phase.

Results presented in Fig.6 confirm that initiation and propagation mechanisms of cathode and anode regime involve very different processes. The cathode regime requires the formation of a gas phase before the propagation of the streamers whereas no presence of vaporization at the cathode has been evidenced for the anode regime.

Conclusion

Number of studies have looked after pre-breakdown and breakdown phenomena in water but most of them have dealt with pin-to-plane configuration or with bubble assistance. These studies have highlighted different regimes of discharge

propagation that are strongly related to the experimental conditions (*e.g.* polarity). Due to this strong correlation, a study of a new configuration, as proposed in this paper (pin-to-pin discharge without bubble), is of great interest. The comparison of the results obtained with different configurations is very helpful to make progress on the understanding of processes. This work has provided new experimental insights into plasma-liquid physics by reporting the study of pin-to-pin underwater discharges by the confrontation of optical diagnostics and electrical measurements. Time resolved measurements have been carried out on a single discharge thanks to high speed detector. This approach is especially important when considering the results of this work which show that different types of discharges can exist for same experimental conditions. This original paper has shown that despite unique set of experimental conditions, the pin-to-pin discharge in water propagates according to three cases and two different regimes: cathode regime (with and without breakdown) and anode regime. Both pre-breakdown and breakdown phenomena have been studied.

Concerning the pre-breakdown, the results have confirmed that the instantaneous power is the same for the three cases but the energy and the charge change. The pre-breakdown RLC current is about 100 mA for all the cases and is monitored before the gas phase apparition. As a consequence we can state that this current is a characteristic of the charge transfer in the liquid phase. The characteristic times evolution is very different for the 2 regimes highlighting different initiation mechanisms. The cathode and anode regimes show high similarities with negative and positive discharges obtained by a pin-to-plane configuration. But unlike positive streamers which show a lower breakdown voltage than negative streamer, the anode regime involves higher breakdown voltage than the cathode regime. For cathode regime, the formation of low density regions in the liquid due to Joule effect, resulting in transient current play an important role in the breakdown process. On the contrary, the anode regime, which does not show either transient signal or gas phase at the cathode, is related to field assisted ionic dissociation. Regarding the cathode regime, the time analysis of the transient current highlights that a faster vaporization favors the breakdown, and the propagation mechanisms control the breakdown.

In case of breakdown, secondary breakdowns phenomena can be observed due to long pulse duration, up to 3 additional breakdowns could occur for cathode regime whereas several additional breakdowns systematically occur for anode regime. For cathode regime, we have shown a correlation between the charge and the number of breakdowns. When less charge is transferred during the pre-breakdown, a higher amount of charge is involved in the breakdown which induces a higher excitation/ionization of the species and then favors more additional breakdowns. The breakdown voltage and the current peak, represented on the (I/V) characteristic, provide very interesting insights for the discharge regime study. The results confirm the theory that for cathode regime low density region is necessary for the electron propagation contrary to the anode regime.

Although the present analysis of the pre-breakdown phenomena is limited by the time resolution of the devices, this paper provides strong evidence of two regimes of discharge for underwater pin-to-pin discharge. It has been established that different types of discharges can exist for same experimental conditions. The parameters behind these differences remain difficult to identify so new experimental results and/or numerical modeling are necessary to further understand the involved mechanisms responsible for the different cases observed.

ACKNOWLEDGMENTS

The authors wish to thank Université Paris 13 for the financial support and Vision Research Company for the large assistance regarding the use of their equipment.

REFERENCES

1. Chadband WG, Wright GT. A pre-breakdown phenomenon in the liquid dielectric hexane. British Journal of Applied Physics. 1965;16(3):305.

2. Fuhr J, Schmidt WF, Sato S. Spark breakdown of liquid hydrocarbons. I. Fast current and voltage measurements of the spark breakdown in liquid n-hexane. Journal of Applied Physics. 1986;59(11):3694-701.

3. Lewis TJ. Basic electrical processes in dielectric liquids. IEEE Transactions on dielectrics and electrical Insulation. 1994;1(4):630-43.

4. Belmonte T, Arnoult G, Henrion G, Gries T. Nanoscience with non-equilibrium plasmas at atmospheric pressure. Journal of Physics D: Applied Physics. 2011;44(36):363001.

5. Graham WG, Stalder KR. Plasmas in liquids and some of their applications in nanoscience. Journal of Physics D: Applied Physics. 2011;44(17):174037.

6. Saito G. Solution Plasma Synthesis of Nanomaterials: Hokkaido University; 2014.

7. Chen Q, Li J, Li Y. A review of plasma–liquid interactions for nanomaterial synthesis. Journal of Physics D: Applied Physics. 2015;48(42):424005.

8. Locke BR. Environmental Applications of Electrical Discharge Plasma with Liquid Water : A Mini Review International Journal of Plasma Environmental Science & Technology. 2012;6(3):194-203.

9. Joshi RP, Thagard SM. Streamer-Like Electrical Discharges in Water: Part II. Environmental Applications. Plasma Chemistry and Plasma Processing. 2013;33(1):17-49.

10. Jiang B, Zheng J, Qiu S, Wu M, Zhang Q, Yan Z, et al. Review on electrical discharge plasma technology for wastewater remediation. Chemical Engineering Journal. 2014;236:348-68.

11. Šunka P. Pulse electrical discharges in water and their applications. Physics of Plasmas. 2001;8(5):2587-94.

12. Foster JE. Plasma-based water purification: Challenges and prospects for the future. Physics of Plasmas. 2017;24(5):055501.

13. Ushakov V, Y., Klimkin, V.F., Korobeynikov, S.M. Impulse breakdown of liquids. systems p, editor: Berlin: Springer; 2007.

14. Bruggeman PJ, Kushner MJ, Locke BR, Gardeniers JGE, Graham WG, Graves DB, et al. Plasma–liquid interactions: a review and roadmap. Plasma Sources Science and Technology. 2016;25(5):053002.

15. Lesaint O. Prebreakdown phenomena in liquids: propagation 'modes' and basic physical properties. Journal of Physics D: Applied Physics. 2016;49(14):144001.

16. Bruggeman P, Leys C. Non-thermal plasmas in and in contact with liquids. Journal of Physics D: Applied Physics. 2009;42(5):053001.

17. Bruggeman P, Walsh JL, Schram DC, Leys C, Kong MG. Time dependent optical emission spectroscopy of sub-microsecond pulsed plasmas in air with water cathode. Plasma Sources Science and Technology. 2009;18(4):045023.

18. Bruggeman P, Verreycken T, González MÁ, L. Walsh J, Kong MG, Leys C, et al. Optical emission spectroscopy as a diagnostic for plasmas in liquids: opportunities and pitfalls. Journal of Physics D: Applied Physics. 2010;43(12):124005.

19. Farazmand B. Study of electric breakdown of liquid dielectrics using Schlieren optical techniques. British Journal of Applied Physics. 1961;12(5):251.

20. Lewis TJ. An overview of Electrical Processes leading to dielectric breakdown of liquids. In: Kunhardt EE, Christophorou LG, Luessen LH, editors. The Liquid State and Its Electrical Properties. Boston, MA: Springer US; 1988. p. 519-37.

21. Clements JS, Sato M, Davis RH. Preliminary Investigation of Prebreakdown Phenomena and Chemical Reactions Using a Pulsed High-Voltage Discharge in Water. IEEE Transactions on Industry Applications. 1987;IA-23(2):224-35.

22. Locke BR, Sato M, Sunka P, Hoffmann MR, Chang JS. Electrohydraulic Discharge and Nonthermal Plasma for Water Treatment. Industrial & Engineering Chemistry Research. 2006;45(3):882-905.

23. Kolb JF, Joshi RP, Xiao S, Schoenbach KH. Streamers in water and other dielectric liquids. Journal of Physics D: Applied Physics. 2008;41(23):234007.

24. Starikovskiy A, Yang Y, Cho Y, I., Fridman A. Non-equilibrium plasma in liquid water: dynamics of generation and quenching. Plasma Sources Science and Technology. 2011;20(2):024003.

25. Marinov I, Guaitella O, Rousseau A, Starikovskaia SM. Cavitation in the vicinity of the high-voltage electrode as a key step of nanosecond breakdown in liquids. Plasma Sources Science and Technology. 2013;22(4):042001.

26. Joshi RP, Thagard SM. Streamer-Like Electrical Discharges in Water: Part I. Fundamental Mechanisms. Plasma Chemistry and Plasma Processing. 2013;33(1):1-15.

27. Joshi RP, Kolb JF, Xiao S, Schoenbach KH. Aspects of Plasma in Water: Streamer Physics and Applications. Plasma Processes and Polymers. 2009;6(11):763-77.

28. Hebner RE. Measurement of Electrical Breakdown in Liquids. In: Kunhardt EE, Christophorou LG, Luessen LH, editors. The Liquid State and Its Electrical Properties. Boston, MA: Springer US; 1988. p. 519-37.

29. Devins JC, Rzad SJ, Schwabe AJ. Breakdown and prebreakdown phenomena in liquids. Journal of Applied Physics. 1981;52(7):4531-45.

30. Massala G, Lesaint O. Positive streamer propagation in large oil gaps: electrical properties of streamers. IEEE Transactions on dielectrics and electrical Insulation. 1998;5(3):371-81.

31. Lesaint O, Massala G. Positive streamer propagation in large oil gaps: experimental characterization of propagation modes. IEEE Transactions on dielectrics and electrical Insulation. 1998;5(3):360-70.

32. Beroual A, Zahn M, Badent A, Kist K, Schwabe AJ, Yamashita H, et al. Propagation and structure of streamers in liquid dielectrics. IEEE Electrical Insulation Magazine. 1998;14(2):6-17.

33. Marinov I, Guaitella O, Rousseau A, Starikovskaia SM. Modes of underwater discharge propagation in a series of nanosecond successive pulses. Journal of Physics D: Applied Physics. 2013;46(46):464013.

34. Sugiarto AT, Sato M, Skalny J, D. Transient regime of pulsed breakdown in low-conductive water solutions. Journal of Physics D: Applied Physics. 2001;34(23):3400.

35. Ono R, Oda T. Visualization of Streamer Channels and Shock Waves Generated by Positive Pulsed Corona Discharge Using Laser Schlieren Method. Japanese Journal of Applied Physics. 2004;43(1R):321.

36. Nieto-Salazar J, Bonifaci N, Denat A, Lesaint O, editors. Characterization and spectroscopic study of positive streamers in water. Dielectric Liquids, 2005 ICDL 2005 2005 IEEE International Conference on; 2005 26 June-1 July 2005.

37. An W, Baumung K, Bluhm H. Underwater streamer propagation analyzed from detailed measurements of pressure release. Journal of Applied Physics. 2007;101(5):053302.

38. Dang TH, Denat A, Lesaint O, Teissedre G. Degradation of organic molecules by streamer discharges in water: coupled electrical and chemical measurements. Plasma Sources Science and Technology. 2008;17(2):024013.

39. Dobrynin D, Seepersad Y, Pekker M, Shneider M, Friedman G, Fridman A. Non-equilibrium nanosecond-pulsed plasma generation in the liquid phase (water, PDMS) without bubbles: fast imaging, spectroscopy and leader-type model. Journal of Physics D: Applied Physics. 2013;46(10):105201.

40. Ceccato PH, Guaitella O, Rabec Le Gloahec M, Rousseau A. Time-resolved nanosecond imaging of the propagation of a corona-like plasma discharge in water at positive applied voltage polarity. Journal of Physics D: Applied Physics. 2010;43(17):175202.

41. Li XD, Liu Y, Zhou GY, Liu SW, Li ZY, Lin FC. Subsonic streamers in water: initiation, propagation and morphology. Journal of Physics D: Applied Physics. 2017;50(25):255301.

42. Akiyama A. Streamer discharges in liquids and their applications. IEEE Transactions on dielectrics and electrical Insulation. 2000;7(5).

43. Nieto-Salazar J, Lesaint O, Denat A, editors. Transient current and light emission associated to the propagation of pre-breakdown phenomena in water. 2003 Annual Report Conference on Electrical Insulation and Dielectric Phenomena; 2003 19-22 Oct. 2003.

44. Stelmashuk V. Time-resolved processes in a pulsed electrical discharge in water generated with shock wave assistance in a plate-to-plate configuration. Journal of Physics D: Applied Physics. 2014;47(49):495204.

45. Stelmashuk V. Microsecond Electrical Discharge in Water in Plate-to-Plate Configuration With Nitrogen Bubble Injection. IEEE Transactions on Plasma Science. 2016;44(4):702-7.

46. Sunka P, Babický V, Clupek M, Lukes P, Simek M, Schmidt J, et al. Generation of chemically active species by electrical discharges in water. Plasma Sources Science and Technology. 1999;8(2):258.

47. Takai O. Solution plasma processing (SPP). Pure and Applied Chemistry2008. p. 2003.

48. Bratescu MA, Saito N, Takai O. Redox reactions in liquid plasma during iron oxide and oxide-hydroxide nanoparticles synthesis. Current Applied Physics. 2011;11(5, Supplement):S30-S4.

49. Hayashi Y, Takada N, Kanda H, Goto M. Effect of fine bubbles on electric discharge in water. Plasma Sources Science and Technology. 2015;24(5):055023.

50. Hamdan A, Cha MS. Ignition modes of nanosecond discharge with bubbles in distilled water. Journal of Physics D: Applied Physics. 2015;48(40):405206.

51. Hamdan A, Cha MS. The effects of gaseous bubble composition and gap distance on the characteristics of nanosecond discharges in distilled water. Journal of Physics D: Applied Physics. 2016;49(24):245203.

52. Settles GS. Schlieren and Shadowgraph Techniques: Visualizing Phenomena in Transparent Media: Springer Berlin Heidelberg; 2012.

53. Felici NJ. Blazing a fiery trail with the hounds (prebreakdown streamers). IEEE Transactions on Electrical Insulation. 1988;23(4):497-503.

54. Lesaint O, Gournay P, Tobazeon R. Investigations on transient currents associated with streamer propagation in dielectric liquids. IEEE Transactions on Electrical Insulation. 1991;26(4):699-707.

55. Ceccato P. Filamentary plasma discharge inside water: initiation and propagation of a plasma in a dense medium: Ecole polytechnique; 2010.